

**$^{12}\text{C}$  and  $^{13}\text{C}(\pi^+, p)$  reaction at  $T_\pi = 90$  and 180 MeV**

R. E. Anderson,\* B. Höistad,† R. L. Boudrie, E. W. Hoffman, R. J. Macek, C. L. Morris, and H. A. Thiessen  
*Los Alamos Scientific Laboratory, Los Alamos, New Mexico 87545*

G. R. Smith‡

*University of Colorado, Boulder, Colorado 80309*

J. Källne

*University of Virginia, Charlottesville, Virginia 22903*

(Received 30 April 1980)

The  $(\pi^+, p)$  reaction has been studied at  $T_\pi = 90$  and 180 MeV on  $^{12}\text{C}$ , and at  $T_\pi = 90$  and 170 MeV on  $^{13}\text{C}$ . The resolution was sufficient to resolve many single levels in the residual nuclei, and angular distributions were obtained between laboratory angles of  $10^\circ$  and  $115^\circ$ . A comparison between the present  $(\pi, p)$  data and existing high-energy  $(p, d)$  data in terms of a model assuming intermediate pion exchange in the  $(p, d)$  reaction indicates that the  $(\pi, p)$  reaction is an important subprocess in the  $(p, d)$  reaction. The present data also suggest that pion rescattering is likely to be a fundamental part of the  $(\pi, p)$  reaction mechanism.

NUCLEAR REACTIONS  $^{12}\text{C}(\pi^+, p)^{11}\text{C}$ ,  $^{13}\text{C}(\pi^+, p)^{12}\text{C}$ ,  $E_\pi = 0.0$  to 28 MeV,  $T_\pi = 90^\circ$  and 170 or 180 MeV,  $\Delta E = 400$  to 600 keV, enriched targets, magnetic spectrometer, measured  $d\sigma/d\Omega(\pi^+, p)$  from  $\theta_{\text{lab}} = 10^\circ$  to  $\theta_{\text{lab}} = 115^\circ$ , comparison with  $(p, d)$  reaction data, reaction mechanism.

## I. INTRODUCTION

Pion absorption reactions are essential processes to understand to be able to describe pion nucleus interactions in a microscopic fashion. In addition, these processes may substantially influence our understanding of other nuclear reactions at intermediate energies. The  $(p, \pi)$  and  $(\pi, p)$  reactions to discrete final states represent rare modes of production and absorption of pions due to the large momentum which is transferred to the residual nucleus. Higher order momentum sharing processes and off-shell effects such as rescattering can, therefore, be an important ingredient of the reaction mechanism itself. Previous experimental data, which exist mainly for the  $(p, \pi)$  reaction,<sup>1</sup> show a great variety in the magnitudes of the differential cross sections and in the shapes of the angular distributions for different nuclear transitions in addition to pronounced sensitivity to the bombarding energy. A hope is therefore nourished that, in spite of the possibility for a complex reaction mechanism, the  $(p, \pi)$  and  $(\pi, p)$  data can give new important information on pion nucleus interactions and nuclear structure when large momenta are involved.

Until recently, the bulk of the available pion production data on complex nuclei has been obtained in the threshold region ( $T_p = 150$ –200 MeV) at Uppsala,<sup>2–8</sup> at Indiana University,<sup>5,6</sup> at Orsay,<sup>7</sup>

and at TRIUMF.<sup>8</sup> Data at higher bombarding energies (400–800 MeV) have been obtained at Saclay<sup>9–11</sup> and recently at LAMPF.<sup>12</sup> Some  $(\pi^+, p)$  data have also been published,<sup>13–15</sup> although these data are generally of rather poor quality due to the energy resolution and the statistics in these experiments. A study of the  $(\pi^-, n)$  reaction on  $^3\text{He}$  and  $^4\text{He}$  has been performed at the energies 100, 200, and 290 MeV.<sup>16</sup>

A large amount of theoretical work has been devoted to the interpretation of various parts of these data.<sup>17</sup> However, a series of difficulties are encountered in these calculations due to ambiguities in the theoretical formalism such as poor knowledge of how to deal with pion rescattering and a large freedom in the choice of parameters determining the nuclear wave functions at large momenta. In addition, the fits to the experimental data are generally not very convincing. Therefore, we must conclude that the reaction mechanism for the  $(p, \pi)$  or  $(\pi, p)$  reactions is largely unknown. There is some evidence for pion rescattering being an important part of the reaction mechanism itself.<sup>18</sup> That is, direct pion emission or absorption is unlikely, but very little is known about the details in the rescattering process. Lacking the fundamental knowledge about the reaction mechanism, it is not possible to tell to what extent the nuclear structure or the reaction dynamics is reflected in the shapes and mag-

nitudes of the existing angular distributions. The aim of the present work is to contribute high quality data so that a better understanding of the basic reaction mechanism of the  $(\pi, p)$  reaction may be achieved.

We have studied the  $^{12,13}\text{C}(\pi^+, p)^{11,12}\text{C}$  reactions at bombarding energies around and below the  $(3,3)$  resonance with the particular aim of gaining information about the role of the pion rescattering in the  $(\pi, p)$  reaction. The pion energies 90 and 180 MeV used in this experiment correspond to obtaining  $(p, \pi^+)$  data at  $T_p = 240$  and 330 MeV and represent, thereby, an energy region where no previous data exist. In addition, the present experiment is the first measurement of the  $(\pi, p)$  reaction done with high energy resolution, which makes it possible to extract angular distributions for transitions to several individual states. Any selectivity of the  $(\pi, p)$  reaction for transitions to some specific types of nuclear states, e.g., single-particle states, core excited states, etc., will therefore be established.

The present data also enables a new comparison between the  $(\pi, p)$  and  $(p, d)$  reactions based on a model for pion emission and reabsorption in the  $(p, d)$  reaction. Using existing  $^{12}\text{C}(p, d)^{11}\text{C}$  data at 700 MeV from Saclay,<sup>19</sup> strong evidence for a link between the two reactions is presented.

## II. EXPERIMENT AND RESULTS

The experiment was carried out using the EPICS channel and spectrometer system of the Clinton P. Anderson Meson Physics Facility of the Los Alamos Scientific Laboratory. The pion channel provided approximately  $10^8$  positive pions per second at the highest pion energy (180 MeV) used in this experiment. A slightly lower flux was obtained at  $T_\pi = 90$  MeV. The momentum spread of the incident beam was  $\pm 1\%$ . The outgoing particles were momentum analyzed using the EPICS spectrometer and delay line drift chambers at the spectrometer entrance and exit, which provided the trajectory for each event. The rear chambers were followed by a scintillator stack that allowed particle identification by  $dE/dx$  and time-of-flight information. This system gave excellent rejection of contaminating charged particles (primarily deuterons). The incident positive pion beam contained about 10 times more protons than pions but these protons did not reach the detector system when the spectrometer field was set for the  $(\pi, p)$  reaction. Pion beam energies of 90 and 180 MeV correspond to 17 and 42 MeV protons, respectively. The remaining background is due presumably to accidental coincidences in the system or to tiny amounts of impurities in the

target. The background remained very small at all angles studied. Background from neutron and gamma ray events was not detectable.

Protons corresponding to a momentum range of 14% in  $\Delta p/p$  were accepted at each spectrometer setting. The acceptance of the spectrometer was measured as a function of position on the focal plane. A decrease of 50% in the acceptance was found at the ends of the momentum bite used in this experiment but a much smaller change was found over most of the active region. The full angular acceptance of the EPICS spectrometer was  $3.5^\circ$  in the scattering plane.

Thin targets were used at some angles forward of  $40^\circ$ , while thicker targets were used at all angles equal to or greater than  $50^\circ$  due to the decreased proton yield. At several scattering angles both the thin and thick targets were used at separate times. This data provided a check on the relative  $^{13}\text{C}$  target thicknesses. All targets measured 15 by 23 cm. The  $^{12}\text{C}$  targets were 228 and 476 mg/cm<sup>2</sup> thick and consisted of natural carbon. The thin  $^{13}\text{C}$  target (208 mg/cm<sup>2</sup>) was manufactured using 99% enriched elemental carbon bonded by  $^{13}\text{C}$  enriched polyethylene binder. The thick  $^{13}\text{C}$  target (396 mg/cm<sup>2</sup>) was enriched to 90%. Where applicable, the  $^{13}\text{C}$  yields have been corrected for the  $^{12}\text{C}$  contamination of the target.

The pion beam was monitored in two ways. First, an ion chamber placed 45 cm downstream from the target observed all of the incident beam. A 1.5-cm thick iron absorber on the face of the ion chamber prevented protons in the incident pion beam from being counted. The ion chamber was sufficiently downstream that it did not contribute to any background in the spectra. Second, the intensity of the primary proton beam on the pion production target was recorded. The two methods gave consistent results. The absolute normalization was obtained by measuring the  $\pi^+ + d \rightarrow p + p$  reaction at several angles for the relevant energies and using published cross sections.<sup>20</sup> The absolute normalization obtained in this manner agrees with that obtained from the (approximately) known pion flux, detector efficiency, and solid angle. Our determination of the absolute cross sections is accurate to  $\pm 20\%$ .

Data were obtained for the  $^{12}\text{C}(\pi^+, p)^{11}\text{C}$  reaction at  $T_\pi = 90$  and 170 MeV. For  $^{12}\text{C}$  at  $T_\pi = 90$  and 180 MeV and for  $^{13}\text{C}$  at  $T_\pi = 90$  MeV data were collected between laboratory angles of  $10^\circ$  and  $115^\circ$  while for  $^{13}\text{C}$  at  $T_\pi = 170$  MeV the data collection stopped at  $80^\circ$ . Minimum cross sections of about  $0.1 \mu\text{b/sr}$  were measured. Representative spectra obtained for the  $^{12}\text{C}(\pi^+, p)^{11}\text{C}$  and  $^{13}\text{C}(\pi^+, p)^{12}\text{C}$  reactions are shown in Fig. 1.

At forward angles the observed resolution of

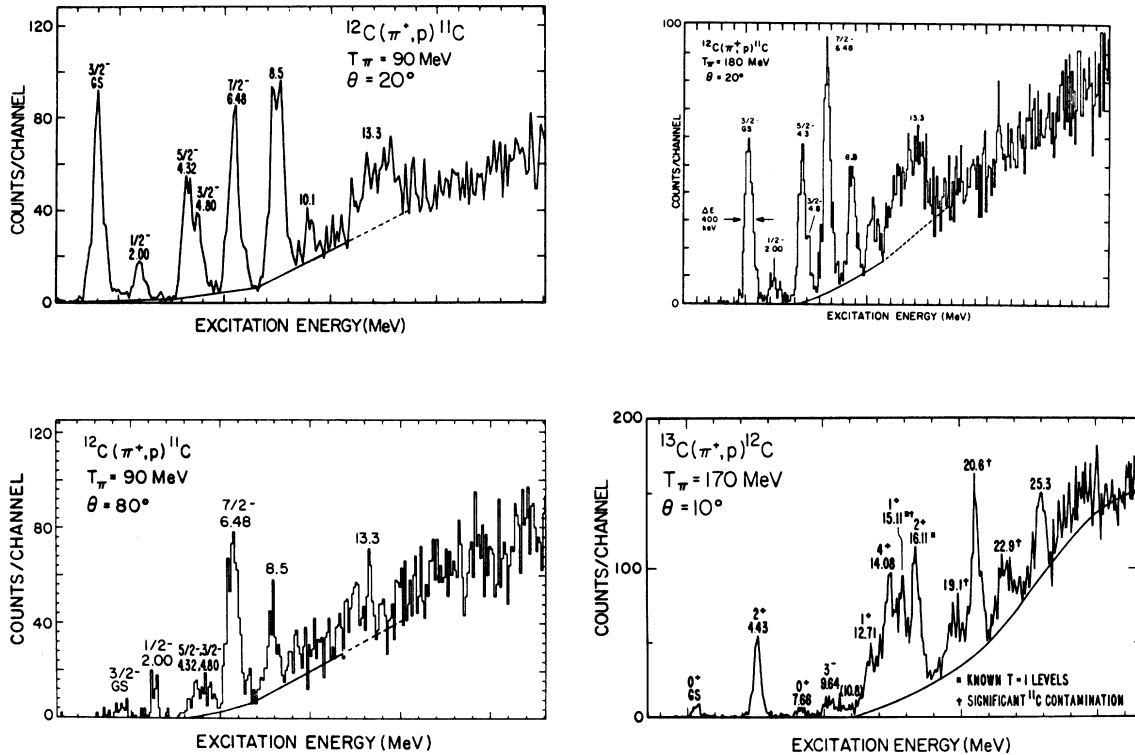


FIG. 1. Spectra obtained for the  $^{12}\text{C}(\pi^+, p)^{11}\text{C}$  reaction at  $T_\pi = 90$  and  $180$  MeV, for the  $^{13}\text{C}(\pi^+, p)^{12}\text{C}$  reaction at  $T_\pi = 170$  MeV. The solid lines are representative fits for the background and the dashed line is the linear background assumed for the  $13.3$  MeV level in  $^{11}\text{C}$ .

400 keV was dominated by target thickness effects and by proton multiple scattering in various windows. For all scattering angles the target angle was set at  $55^\circ$  with respect to the beam in order to minimize the energy loss difference between protons and pions. The resolution at the backward angles deteriorated to about 600 keV due to the use of the thicker targets. All data were obtained using transmission geometry. Identification of the observed peaks with known states in  $^{11}\text{C}$  and  $^{12}\text{C}$  (Ref. 21) was based on the measured excitation energies. Good agreement was found between measured and tabulated energies for most of the peaks. For the few peaks which could not be unambiguously identified with known levels, the excitation energies were determined from the measured proton momentum. Uncertainties in the excitation energies of these levels were determined by comparisons with the excitation energies obtained from fits to peaks with well known excitation energies.

For a number of spectra the areas for individual peaks were extracted by two line shape fitting routines and several different line shapes were assumed. The simplest procedure involved use of a Gaussian line shape with variable width,

height, and centroid. A modification of this routine used an asymmetric Gaussian with width and asymmetry fixed based upon either the  $^{11}\text{C}(\text{g.s.})$  or  $^{12}\text{C}(4.43)$  level. A second routine used an experimental peak shape which was again either the  $^{11}\text{C}(\text{g.s.})$  or  $^{12}\text{C}(4.43)$  shape depending on the target. The height and centroid were permitted to vary. For the strong peaks where little background was present (e.g., most levels in  $^{11}\text{C}$  at or below 8.5 MeV excitation and levels in  $^{12}\text{C}$  at or below 16.1 MeV excitations) the various procedures were in excellent agreement and the errors given in the figures are dominated by counting statistics. For weaker states (the 2.00 MeV level in  $^{11}\text{C}$ ) or for strong states which sit on a large background (the levels between 20 and 25 MeV excitation in  $^{12}\text{C}$ ), the uncertainties in the background fits dominated the uncertainties in the peak areas. Three parameter polynomial backgrounds which conformed to the average shape of the spectra were assumed, and typical background fits are shown in Fig. 1. For the  $13.3$  MeV level in  $^{11}\text{C}$ , the total number of counts in the region was used because of its odd peak shape, and a linear background was assumed for that peak as indicated in Fig. 1. The errors given

in the figures include statistical errors, fitting errors, and errors due to the background subtraction.

### III. DISCUSSION OF EXPERIMENTAL RESULT

#### A. General characteristics of the $(\pi, p)$ spectra

The salient features in the  $(\pi, p)$  spectra can be deduced from Fig. 1 in which typical spectra from the  $^{12}\text{C}(\pi, p)^{11}\text{C}$  and  $^{13}\text{C}(\pi, p)^{12}\text{C}$  reactions are presented. A large number of levels in the residual nuclei are excited, and essentially all known low-lying excited states<sup>21</sup> in  $^{11}\text{C}$  and  $^{12}\text{C}$  are populated.

The transitions to states with single particle configurations are prominent in the  $(\pi, p)$  spectra. The ground state ( $1p_{3/2}$  hole) and the 2.0 MeV ( $1p_{1/2}$  hole) levels in  $^{11}\text{C}$  are populated with a ratio of 4.5:1 at forward angles, which is in agreement with spectroscopic factors obtained from  $(p, d)$  work.<sup>22</sup> In contrast, the ratio of the ground state and the 4.8 MeV ( $3/2^-$ ) level deviates from this simple expectation. The latter level contains about 7% of the  $p_{3/2}$  single particle strength as well as a strong  $[2^+ \otimes p_{3/2}^{-1}]_{3/2^-}$  component. The 4.3 and 4.8 MeV levels could not always be separated, but the spectra shown in Fig. 1 are of sufficient quality to permit a reliable separation to be made. The spectrum obtained at 90 MeV indicates that the cross section for the transition to the 4.8 MeV state is  $29 \pm 4\%$  of that of the transition to the ground state, which is roughly a factor of four larger than the ratio of the corresponding single particle strengths. At  $T_\pi = 180$  MeV, a ratio of  $14 \pm 5\%$  is obtained. These facts show that the  $(\pi, p)$  reaction is not likely to be a simple pickup process. Moreover, the transitions to the core excited states in  $^{11}\text{C}$  are generally strong, which can be exemplified by the large cross sections for populating the 4.3 and 6.48 MeV states which are the  $\frac{5}{2}^-$  and  $\frac{7}{2}^-$  members of the  $(2^+ \otimes p_{3/2}^{-1})$  multiplet.

The  $(\pi, p)$  spectrum in Fig. 1 reveals a broad bump at 13.3 MeV in  $^{11}\text{C}$ , which has not been observed before. Very little is known about the states around 13 MeV excitation energy in  $^{11}\text{C}$ , so it is an open question what causes the  $(\pi, p)$  reaction to be selective for existing states in this energy region. Available  $(p, d)$  data at 800 MeV (Ref. 23) does have this bump. Previous  $^{12}\text{C}(\pi, p)^{11}\text{C}$  data<sup>15</sup> obtained at 49 MeV show a somewhat different behavior in this region since a sharp state, with a width corresponding to the experimental energy resolution of 1.65 MeV, is seen at  $12.5 \pm 0.3$  MeV. This peak was suggested in Ref. 15 to be identified with the  $\frac{1}{2}^-$ ,  $T = \frac{3}{2}$  state at 12.5 MeV. The difference in the  $^{12}\text{C}(\pi, p)$  spectra

obtained at 49 and 90 MeV with respect to the 12–14 MeV region persists when the comparison is done at the same momentum transfer. No other prominent states are seen in the  $^{11}\text{C}$  spectrum up to an excitation energy of 40 MeV. We therefore do not find any evidence at either  $T_\pi = 90$  or 180 MeV for any preferred population of states in  $^{11}\text{C}$  which would involve  $T = \frac{3}{2}$  transfer. The same conclusion can be drawn from the  $^{13}\text{C}(\pi, p)$  data both at 90 and 170 MeV in the sense that no known  $T = 2$  states are seen in  $^{12}\text{C}$ . Of course  $\Delta T = \frac{3}{2}$  transfer could be involved in the population of  $T = 1$  states in  $^{12}\text{C}$ , and Sec. IIIC below discusses this in more detail.

An interesting remark can be made concerning the low resolution measurement of the  $^{16}\text{O}(\pi, p)^{15}\text{O}$  reaction at 66 MeV done by Bachelier *et al.*<sup>14</sup> In that work they found the ratio of the cross sections for the transitions to the  $1p_{3/2}$  and  $1p_{1/2}$  one-hole states to be 10:1, which is in sharp contrast to the ratio 2:1 obtained from low energy pickup reactions as well as to our  $(\pi, p)$  results from  $^{12}\text{C}$ . In view of the strong excitation of the core coupled states in  $^{11}\text{C}$  via the  $(\pi, p)$  reaction, it is probable that the cross section for the excitation of the  $[3^- \otimes p_{1/2}^{-1}]$  states at 5.24 and 7.28 MeV is not negligible as assumed in Ref. 14 and the ratio thus would be 10:1; only a very rough upper limit.

#### B. General features in the angular distributions

The angular distributions from transitions to individual states or group of states in the  $^{12}\text{C}(\pi, p)^{11}\text{C}$  and  $^{13}\text{C}(\pi, p)^{12}\text{C}$  reactions are presented in Figs. 2 and 3. These distributions reveal a remarkable similarity in shape for many of the transitions and with few exceptions, there are no distinct features to be associated with the structure of the initial or final nuclear state. In particular, at angles below  $70^\circ$  all angular distributions show a uniform fall off with angle. In view of the great variety in the shapes of the angular distributions seen in the  $(p, \pi)$  data, this might be surprising. It should be pointed out, however, that our  $(\pi, p)$  data are obtained at energies closer to the (3, 3) resonance than previous  $(p, \pi)$  data. We observe that the  $(\pi, p)$  angular distributions obtained at 180 MeV are even more featureless than those obtained at 90 MeV. The present data thus indicate that the approach of the (3, 3) resonance leads to a suppression of the structure in the angular distributions from transitions in the  $(\pi, p)$  reaction.

From a closer examination of the angular distributions presented in Figs. 2 and 3 we can make some interesting remarks. One is found in the angular distribution for the  $^{12}\text{C}(\pi, p)^{11}\text{C}(\text{g.s.})$  transition (Fig. 2), which contains a deep mini-

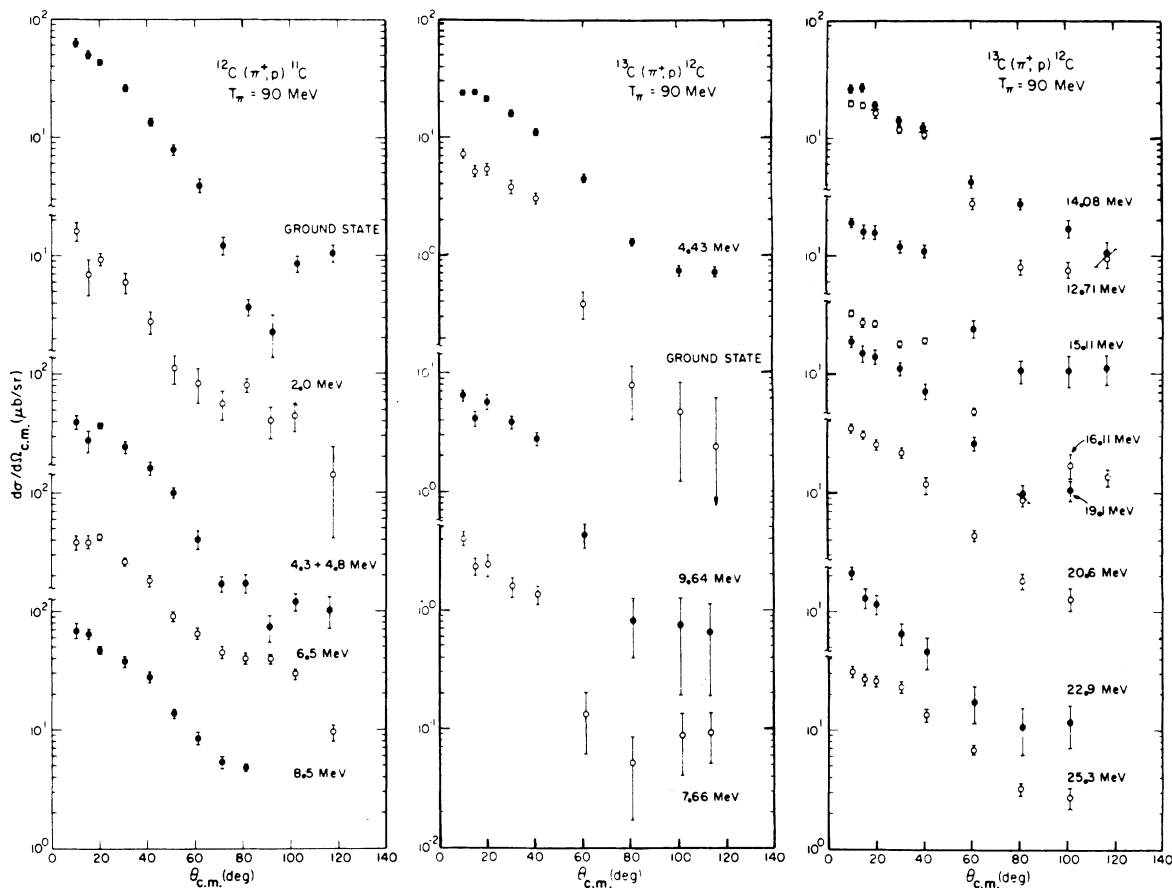


FIG. 2. Angular distributions obtained in the  $^{12,13}\text{C}(\pi^+, p)$  reactions at  $T_\pi = 90$  MeV.

imum around  $85^\circ$ . This is the only transition which gives rise to a pronounced minimum in the angular range studied here. In contrast, essentially no structure is seen in the distribution for the  $^{13}\text{C}(\pi, p)^{12}\text{C}^*(4.4 \text{ MeV}; 2^+)$  transition, shown in Fig. 3, which also involves removal of a  $1p_{3/2}$  neutron. We also note that the  $^{13}\text{C}(\pi, p)^{12}\text{C}(\text{g.s.})$  transition lacks a distinct minimum in the angular distribution, and that the cross section is about 8–10 times smaller (for  $\theta_p < 80^\circ$ ) than the cross section from the  $^{12}\text{C}(\pi, p)^{11}\text{C}(\text{g.s.})$  reaction. This is half the magnitude expected from a direct pickup process.

Most of the angular distributions obtained at 90 MeV show a more or less pronounced shoulder around  $80^\circ$ . This inflection point should perhaps not be associated with any type of nuclear structure since it occurs in transitions to states which involve a large single particle component as well as to pure core excited states. The core excited levels in  $^{11}\text{C}$  at 4.3+4.8 MeV, and 6.5 MeV, show almost identical angular distributions characterized by a shoulder near  $90^\circ$ . The distribution for

the 8.5 MeV level is consistent with this shape, although the state could not be observed beyond  $80^\circ$ . The excited levels in  $^{12}\text{C}$  show a slightly different behavior since a minimum or a plateau is reached near  $90^\circ$ . The one exception to this shape is seen for the 14.08 MeV transition which has a shape more closely resembling the core excited levels in  $^{11}\text{C}$ . The angular distribution for the transition to the unidentified bump at 13.3 MeV in  $^{11}\text{C}$  does not show any significant deviation from a straight slope.

At 180 and 170 MeV there is much less variation in the shapes of the angular distributions. The pronounced minimum in the  $^{12}\text{C}(\pi, p)^{11}\text{C}(\text{g.s.})$  data of 90 MeV survives only as a hint of an inflection point.

### C. The energy variation in the $(\pi, p)$ reaction

Data on the energy variation in the  $(\pi, p)$  reaction is very scarce. In particular, there is a lack of data from target nuclei heavier than  $^4\text{He}$  at energies close to the (3, 3) resonance. This energy region is of special interest because of

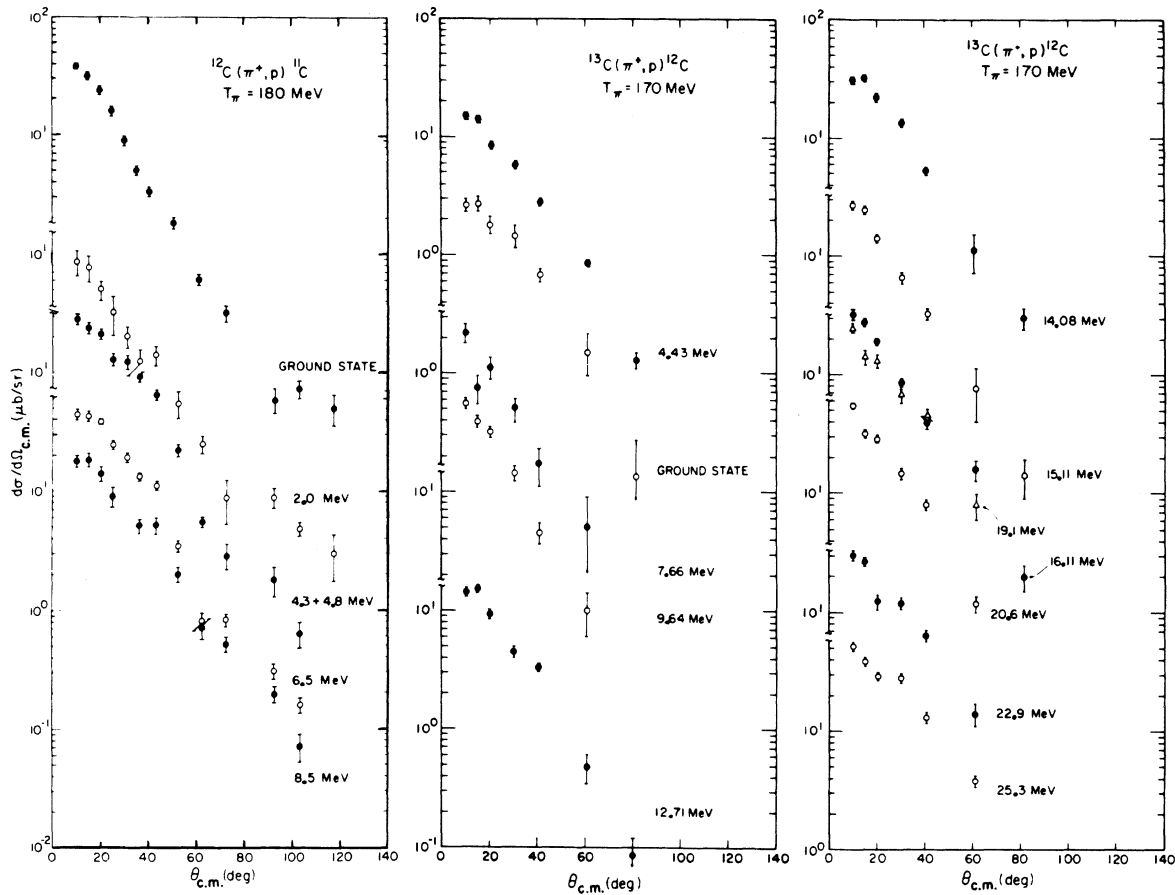


FIG. 3. Angular distributions obtained in the  $^{12}\text{C}$ ,  $^{13}\text{C}(\pi^+, p)$  reactions at  $T_\pi = 180$  or  $170$  MeV.

the rapid energy variation in the pion-nucleon interaction. This variation presents an opportunity to learn how an increase in the pion rescattering will be reflected in the  $(\pi, p)$  data.

Qualitatively the relative magnitudes of the forward angle cross sections for transitions to different levels in  $^{11}\text{C}$  remain unaffected. One exception is found in  $^{11}\text{C}$ , where the transition to the 8.5 MeV level which decreases in intensity relative to transitions to the other levels as the pion energy is decreased. The levels in  $^{12}\text{C}$  exhibit a much more varied behavior.

Figure 4 shows the angular distributions for the  $^{11}\text{C}$  ground state obtained at  $T_\pi = 50, 90,$  and  $180$  MeV plotted as a function of momentum transfer. We observe that the minimum in the angular distribution obtained at  $90$  MeV, and the shoulders in the distributions obtained at  $50$  and  $180$  MeV occur at very different momentum transfer. It is therefore unlikely that the structure in these distributions is directly related to the nuclear wave function. This conclusion is based on the assumption that the reaction mechanism remains

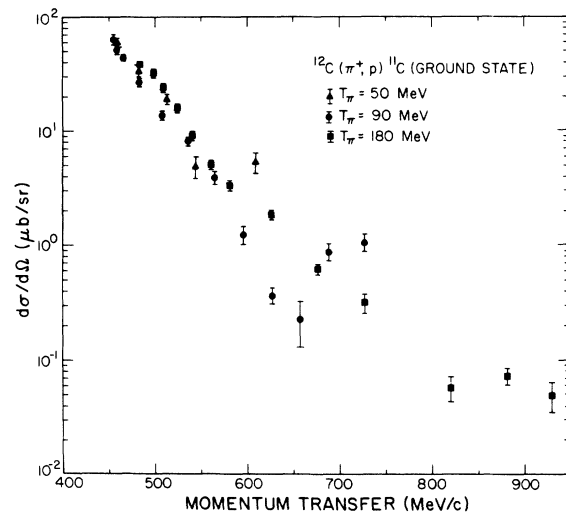


FIG. 4. Momentum transfer distributions for the  $^{12}\text{C}(\pi^+, p)^{11}\text{C}(\text{g.s.})$  reaction at  $T_\pi = 50, 90,$  and  $180$  MeV. The first minimum (or inflection point) in the distributions can be seen to move from approximately  $575$  MeV/c at  $T_\pi = 50$  MeV to approximately  $650$  MeV/c and  $825$  MeV/c at  $T_\pi = 90$  and  $180$  MeV, respectively.

the same in the considered energy interval, so that the same part of the wave function is probed at all pion energies. The last two points in the 50 MeV data are obtained at  $75^\circ$  and  $100^\circ$  which cover the angular region in which the dip occurs in the 90 MeV data and the shoulder in the 180 MeV data. This shows that the structure in the angular distribution occurs at approximately the same angle independent of bombarding energy. Such a characteristic in the data is expected if  $p$ -wave pion rescattering is a part of the reaction mechanism.<sup>24,25</sup> The present  $(\pi, p)$  data suggest that pion rescattering is an important ingredient in the  $(\pi, p)$  reaction mechanism.

Apart from studying the energy dependence in the shape of the angular distribution, we can get further insight into the reaction mechanism by studying the energy dependence of the magnitude of the  $(\pi, p)$  cross section to a specific final state. Although data are not available for the total  $(\pi, p)$  cross section we can get a reasonably realistic picture of the energy variation by studying the cross section at a fixed momentum transfer for all energies. The influence from the nuclear structure should remain approximately the same for all energies, and the data should display the energy-dependence of only the reaction mechanism. We assume that the difference in pion distortion at 90 and 180 MeV does not change significantly the region in which the nuclear wave function is probed. In Fig. 5, the  $(\pi, p)$  differential cross sections for several transitions are presented as a function of bombarding energy. The data points are taken at momentum transfers of 510 MeV/c. These are forward angle data ( $20^\circ$  at 180 MeV and  $40^\circ$  at 90 MeV) where all angular distributions have nearly the same slope. In Fig. 5 we see some variation in the energy dependence of the  $(\pi, p)$  reaction, both with respect to the target nucleus and the transition considered. For example, cross sections for the  $^{13}\text{C}(\pi, p)^{12}\text{C}(\text{g.s.})$  and the  $^{12}\text{C}(\pi, p)^{11}\text{C}^*(8.5 \text{ MeV})$  transitions decrease between 90 and 180 MeV, while the cross section for the  $^{12}\text{C}(\pi, p)^{11}\text{C}(\text{g.s. and } 6.5 \text{ MeV})$  transitions increase in the same energy interval.

The 15.11 and 12.71 MeV levels in  $^{12}\text{C}$  are of particular interest since they are the  $1^+$ ,  $T=1$  and  $1^+$ ,  $T=0$  members of the  $(p_{1/2} \otimes p_{3/2}^{-1})$  multiplet. The nuclear structures of the levels are thus expected to be identical except for the isospin difference. At  $T_\pi=90$  MeV the two levels are equally populated, while at  $T_\pi=170$  MeV the 15.1 MeV level is  $55 \pm 14\%$  stronger. Since the 15.1 MeV level may be populated by  $T=\frac{1}{2}$  or  $T=\frac{3}{2}$  transfer while the 12.7 MeV level may be populated only by  $T=\frac{1}{2}$  transfer we may have the

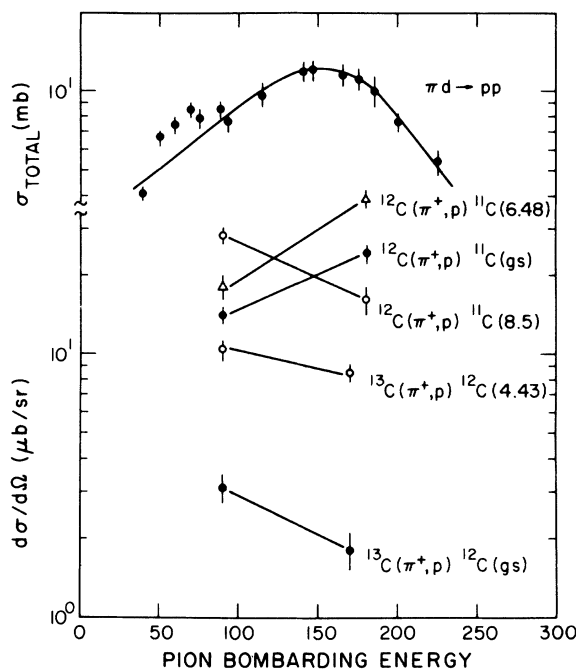


FIG. 5. Forward angle  $(\pi^+, p)$  reaction cross sections for several levels in  $^{12}\text{C}$  and  $^{11}\text{C}$ . Energy dependence for the elementary  $\pi d \rightarrow pp$  process is also presented for comparison.

first indication that  $T=\frac{3}{2}$  transfer is present in the  $(\pi, p)$  reaction.

The irregularities in the energy dependence of the  $(\pi, p)$  transitions suggest not only a much larger sensitivity to the nuclear structure than appeared from the shape of the angular distributions, but also that the interplay between the reaction mechanism and the nuclear structure might be a significant factor in the  $(\pi, p)$  reaction. Since one specific reaction mechanism should show roughly the same energy dependence, at least for transitions of the same general type (single particle, core excited, etc.), we might interpret the individual energy dependence as an indication that the details in the reaction mechanism are affected by the nuclear structure of the final state.

#### D. Comparisons between the $(\pi, p)$ and $(p, d)$ reactions

Recent data on the  $(p, d)$  reaction<sup>19,23,26</sup> at intermediate energies show many similarities with our  $(\pi, p)$  data. Unlike the result from low energy  $(p, d)$  measurements, the data obtained at 700 and 800 MeV do not show any enhancement for transitions to single particle states, but the core-excited states are equally strongly excited. As pointed out earlier this is also a characteristic feature of the  $(\pi, p)$  reaction. In addition, the relative

strength of the different transitions are strikingly similar in the two reactions. This appears clearly from a comparison between the  $(p, d)$  spectra<sup>23</sup> from  $^{12}\text{C}$  and  $^{13}\text{C}$  presented in Fig. 6 and the corresponding  $(\pi, p)$  spectra shown in Fig. 1. Furthermore, these spectra show that the peaks in the 12–16 MeV region of the  $(\pi, p)$  spectra for  $^{11}\text{C}$  also appear in the  $(p, d)$  data. The close resemblance between the  $(\pi, p)$  and  $(p, d)$  data is an indication that the two reactions have some basic common features in the reaction mechanism. The nature of this common process should appear in a comparison between the angular distributions from the same transitions in the  $(\pi, p)$  and  $(p, d)$  reactions. If the two reactions are dominated by a simple pickup process, one would expect the angular distributions to be similar when plotted as a function of momentum transfer. Such a comparison is made in Fig. 7 where the data from the transitions to the ground state and 6.48 MeV state in  $^{11}\text{C}$  are shown as given by  $(\pi, p)$  data at 180 MeV and  $(p, d)$  data<sup>19</sup> at 700 MeV. Although it is not clear at what energy the two reactions should be compared in a pickup model, we choose the  $(\pi, p)$  data at 180 MeV rather than 90 MeV because of a larger overlap in momentum transfer. As seen in Fig. 7, there are significant

differences between the  $(\pi, p)$  and  $(p, d)$  angular distributions for the transitions to the  $^{11}\text{C}(\text{g.s.})$ , and to the 6.48 MeV state. These two cases do not present convincing arguments for a simple pickup process being the common reaction pattern.

It has recently been suggested<sup>27,28</sup> that intermediate pion production becomes more and more important in the  $(p, d)$  reaction when the incident proton energy is increased above the pion production threshold. The Wilkin model<sup>27</sup> can be described by the triangle graph shown in Fig. 8. The pion is emitted from the incident proton and then absorbed in the target nucleus via the  $(\pi, p)$  reaction. The deuteron is formed from the neutron in the  $(p, n)$  vertex and the proton in the  $(\pi, p)$  reaction. In this model, the  $(p, d)$  cross section can be expressed in terms of the measured  $(\pi, p)$  cross section and a function describing the pion emission and propagation. Thus, the  $(\pi, p)$  reaction can be considered as a subprocess to the  $(p, d)$  reaction. This model also contains the important prescription of how the incident energies as well as the scattering angles in the  $(\pi, p)$  and  $(p, d)$  reactions are related. Furthermore, the absolute cross section is normalized by backward elastic proton-deuteron scattering. It is evident that if this model is realistic, one should not expect the angular distributions to be identical if simply compared as a function of momentum transfer. Following the description of Wilkin, one can now calculate the  $(p, d)$  cross sections from our  $(\pi, p)$  data, or since the equations involved are factorized, the inverse process. We have calculated the  $^{12}\text{C}(\pi, p)^{11}\text{C}$  cross sections at  $T_\pi = 180$  MeV from  $(p, d)$  data at the corresponding energy of 625 MeV. Since  $(p, d)$  data on  $^{12}\text{C}$  is not available exactly at 625 MeV, we use as an approximation the existing data at 700 MeV from Saclay.<sup>19</sup> The results are presented in Fig. 9. As can be seen the agreement between the calculated and the measured  $(\pi, p)$  cross section is remarkable for the transitions to the ground state and 6.48 MeV state in  $^{11}\text{C}$ . The same qualitative agreement is found for the transitions to the 2.0 MeV state and the peak containing the 4.3 and 4.8 MeV states in  $^{11}\text{C}$  for which data from both reactions exist. Consequently, clear evidence is found that the  $(p, d)$  and  $(\pi, p)$  reactions are closely related at energies above the pion production threshold. In particular, this link is due to the presence of pion exchange via a  $(\pi, p)$  subprocess in the  $(p, d)$  reaction at intermediate energies. Further experimental data are needed to establish the correspondence between the two reactions. We point out that although the present data result is a substantial contribution toward our understanding of the  $(p, d)$  reaction, the details

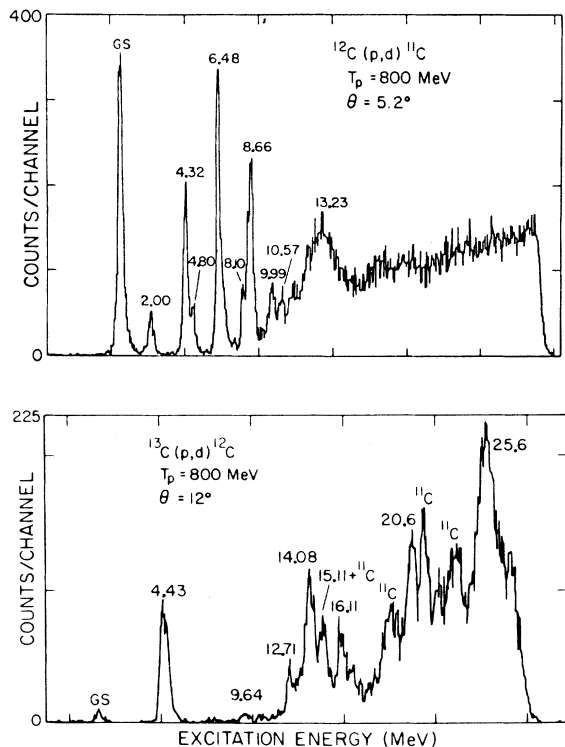


FIG. 6. Typical spectra observed (Ref. 23) in the  $^{12}\text{C}(p, d)^{11}\text{C}$  and  $^{13}\text{C}(p, d)^{12}\text{C}$  reactions at  $T_p = 800$  MeV.

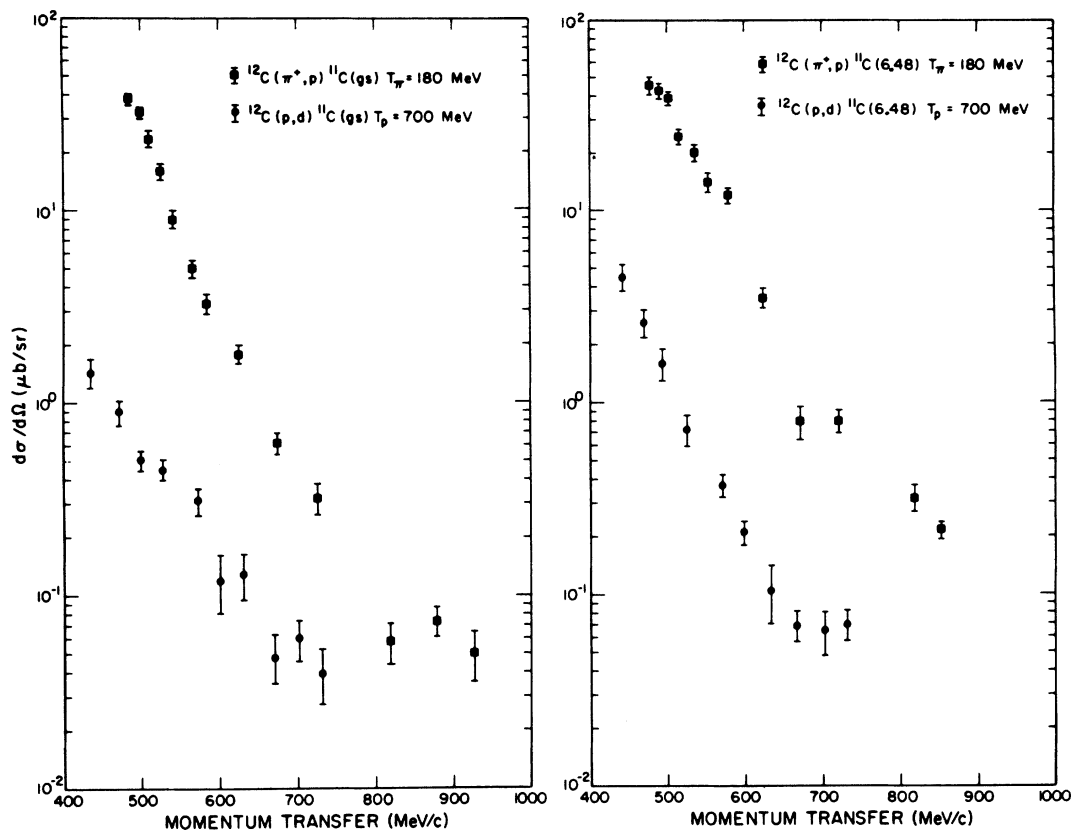


FIG. 7. Momentum transfer distributions for the  $^{11}\text{C}(\text{g.s.})$  and  $^{11}\text{C}(6,48)$  levels as observed in the  $(\pi^+, p)$  reaction at 180 MeV and the  $(p, d)$  reaction (Ref. 19) at 700 MeV.

of the  $(\pi, p)$  reaction are not further elucidated by this model.

#### IV. SUMMARY AND FINAL REMARKS

We have presented high resolution data from the  $(\pi^+, p)$  reaction on  $^{12}\text{C}$  and  $^{13}\text{C}$  at energies close to and below the  $(3, 3)$  resonance.<sup>29</sup> A large number of individual states in the  $(\pi^+, p)$  spectra have been resolved. Both single particle and core excited levels are strongly populated. We have not found

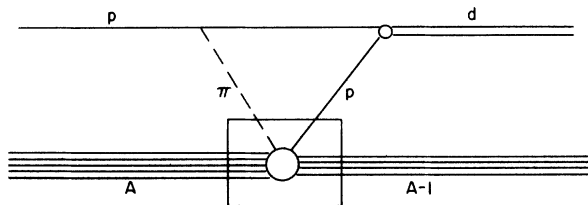


FIG. 8. Schematic representation of the  $A(p, d)A-1$  reaction including pion exchange. The box illustrates the role of the  $(\pi^+, p)$  subprocess in this reaction.

any strong evidence for  $\Delta T = \frac{3}{2}$  transfers, although the energy dependent ratio for the excitation of the 12.7 and 15.1 MeV levels in  $^{12}\text{C}$  may indicate the presence of  $\Delta T = \frac{3}{2}$  transfer. A broad bump around 13.3 MeV excitation energy in  $^{11}\text{C}$  deserves special attention since the excitation of this state is not understood at present. The levels above 16.1 MeV in  $^{12}\text{C}$  should also be mentioned in this context.

Angular distributions for transitions to several individual states in the residual nucleus have been presented. The similarities observed, especially at  $T_\pi = 180$  MeV, suggest large effects due to the reaction mechanism and hence less sensitivity to nuclear structure. In contrast, the energy variation of the  $(\pi, p)$  reaction to different final states show some dependence on the initial and final state of the nuclear transition. These observations suggest a prevailing interplay between the reaction mechanism and the nuclear structure.

Comparison between the present  $(\pi, p)$  data and existing high energy  $(p, d)$  data reveals striking similarities in the relative strengths of the different transitions. A more quantitative analysis of

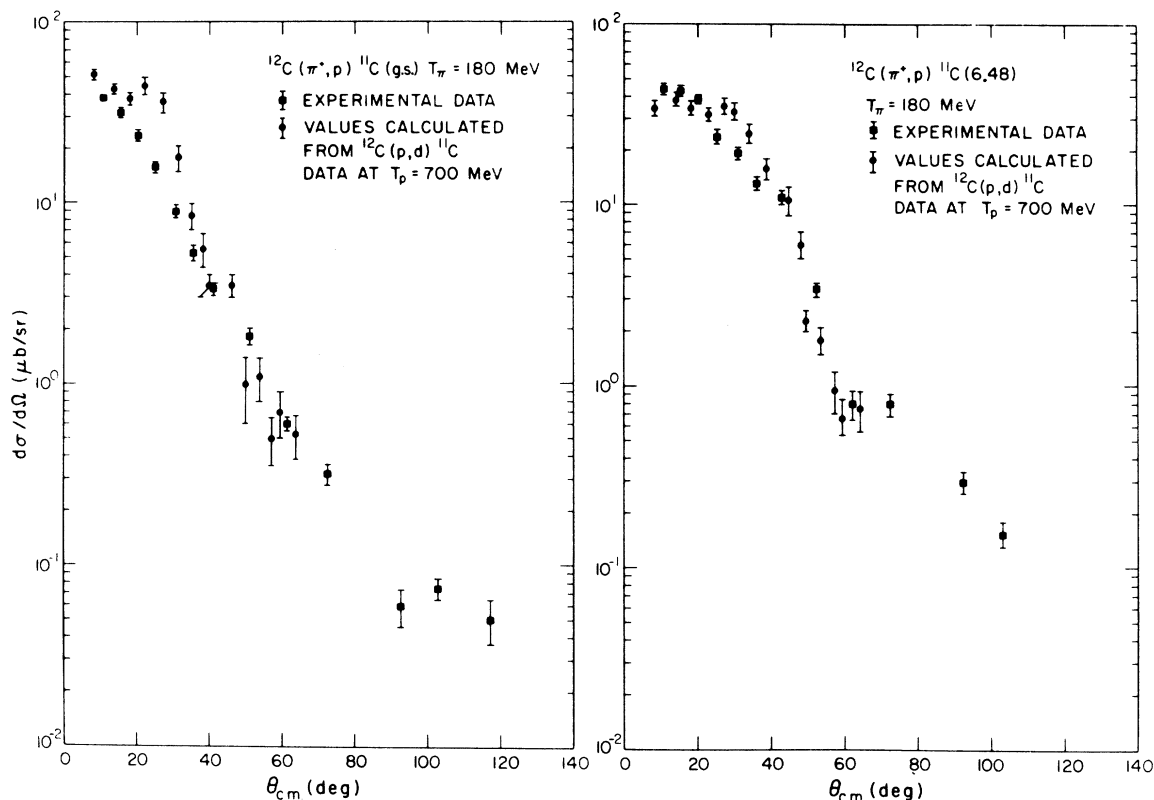


FIG. 9. Angular distributions for the  $^{11}\text{C}(\text{g.s.})$  and  $^{11}\text{C}(6.48)$  levels as seen in the  $(\pi^+, p)$  reaction and as predicted from the 700-MeV proton data, based on Wilkin's model.

these data in terms of a model assuming intermediate pion exchange in the  $(p, d)$  reaction indicates that the  $(\pi, p)$  reaction is a subprocess in the  $(p, d)$  reaction.

The present data give important information about the  $(\pi, p)$  reaction mechanism and suggest that the pion rescattering is likely to be a fundamental part of the reaction mechanism itself. The details of the  $(\pi, p)$  reaction mechanism, i.e., the prevailing dynamics and their role in the sharing of the large transferred momentum, seem to be affected by the initial and final state

of the nuclear transition.

We hope that the present data will help unravel the puzzle surrounding our understanding of the  $(\pi, p)$  reaction. In addition, the data also goes beyond this by indicating relationships to other nuclear reactions such as the  $(p, d)$  reaction. Some form of pion exchange might play a crucial role in nuclear reactions in general among heavier targets and projectiles at equivalent intermediate energies. The  $(\pi, p)$  and  $(p, \pi)$  reactions represent an important case when the pion appears on the mass shell.

\*Present address: Department of Physics and Astronomy, University of North Carolina, Chapel Hill, North Carolina 27514.

†Present address: Department of Physics, University of Texas, Austin, Texas 78712.

‡Present address: Schweizerisches Institut Für Nuklearforschung, CH-5234 Villigen, Switzerland.

<sup>1</sup>The experimental work on the  $(p, \pi)$  reaction is reviewed by: B. Höistad, *Proceedings of the Seventh International Conference on High Energy Physics and Nuclear Structure, Zürich (1977)*, edited by M. P.

Locher (Birkhauser, Basel, 1977); *Advances in Nuclear Physics*, edited by J. Negele and E. Vogt (Plenum, New York, 1978), Vol. II, Chap. 2; E. Aslanides, in *Meson-Nuclear Physics—1976* (Carnegie-Mellon Conference) Proceedings of the International Topical Conference on Meson Nuclear Physics, edited by P. D. Barnes, R. A. Eisenstein, and L. S. Kisslinger (AIP, New York, 1976), D. F. Measday and G. A. Miller, *Ann. Rev. Nucl. Part. Sci.* **29**, 121 (1979).

<sup>2</sup>S. Dahlgren, P. Grafström, B. Höistad, and A. Åsberg, *Phys. Lett.* **35B**, 219 (1971); *ibid.* **47B**, 439 (1973);

- Nucl. Phys. A204, 53 (1973); A211, 243 (1973); A227, 245 (1974).
- <sup>3</sup>B. Höistad, T. Johansson, and O. Jonsson, Phys. Lett. B73, 123 (1978); *ibid.* B79, 385 (1979).
- <sup>4</sup>B. Hoistad, S. Dahlgren, T. Johansson, and O. Jonsson, Nucl. Phys. A319, 409 (1979).
- <sup>5</sup>R. D. Bent *et al.*, Phys. Rev. Lett. 40, 495 (1978).
- <sup>6</sup>P. H. Pile *et al.*, Phys. Rev. Lett. 42, 1461 (1979).
- <sup>7</sup>Y. LeBornec *et al.*, Phys. Lett. 61B, 47 (1976).
- <sup>8</sup>E. Auld *et al.*, Phys. Rev. Lett. 41, 462 (1978).
- <sup>9</sup>B. Tatischeff *et al.*, Phys. Lett. 63B, 158 (1976).
- <sup>10</sup>T. Bauer *et al.*, Phys. Lett. 69B, 433 (1977).
- <sup>11</sup>E. Aslanides *et al.*, Phys. Rev. Lett. 39, 1654 (1977).
- <sup>12</sup>B. Höistad *et al.*, Phys. Rev. Lett. 43, 487 (1979).
- <sup>13</sup>J. Amato *et al.*, Phys. Rev. C 9, 501 (1974).
- <sup>14</sup>D. Bachelier *et al.*, Phys. Rev. C 15, 2139 (1977).
- <sup>15</sup>J. F. Amann *et al.*, Phys. Rev. Lett. 40, 758 (1978).
- <sup>16</sup>J. Källne *et al.*, Phys. Rev. Lett. 40, 378 (1978).
- <sup>17</sup>The theory on the ( $p, \pi$ ) reaction is reviewed by: V. S. Bhasin, Internal Report No. BON-HE-77-22, Bonn University, 1977; J. M. Eisenberg, in *High Energy Physics and Nuclear Structure—1975 (Santa Fe and Los Alamos)*, Proceedings of the Sixth International Conference on High Energy Physics and Nuclear Structure, edited by D. E. Nagle and A. S. Goldhaber (AIP, New York, 1975); M. P. Locher, in *High Energy Physics and Nuclear Structure*, Proceedings of the Fifth International Conference, Uppsala, Sweden, edited by G. Tibell (North-Holland, Amsterdam, 1974); J. V. Noble, in *Meson-Nuclear Physics—1976 (Carnegie-Mellon Conference)*, Proceedings of the International Topical Conference on Meson-Nuclear Physics, edited by P. D. Barnes, R. A. Eisenstein, and L. S. Kisslinger (AIP, New York, 1976); A. Reitan, Report from a talk given at the Symposium on High Energy Reactions in Nuclei, Spåtind, Norway, 1977.
- <sup>18</sup>M. Dillig and M. G. Huber, Nuovo Cimento Lett. 16, 293 (1976); 16, 299 (1976).
- <sup>19</sup>S. D. Baker *et al.*, Phys. Lett. 52B, 57 (1974).
- <sup>20</sup>C. Richard-Serre *et al.*, Nucl. Phys. B20, 413 (1970).
- <sup>21</sup>F. Ajzenberg-Selove, Nucl. Phys. A248, 1 (1975).
- <sup>22</sup>J. Källne and A. W. Obst, Phys. Rev. C 15, 477 (1977).
- <sup>23</sup>C. A. Whitten, Jr., Proceedings of the 8th International Conference on High Energy Physics and Nuclear Structure, Vancouver, 1979 (to be published).
- <sup>24</sup>Z. Grossman, F. Lenz, and M. P. Locker, Ann. Phys. (N.Y.) 84, 348 (1974).
- <sup>25</sup>G. Miller, Nucl. Phys. A224, 269 (1974); T. S. Bauer, *et al.*, Phys. Rev. C 21, 757 (1980).
- <sup>26</sup>J. Källne and E. Hagberg, Phys. Scr. 4, 151 (1971).
- <sup>27</sup>C. Wilkin, J. Phys. G 5, 69 (1980).
- <sup>28</sup>J. Källne and P. C. Gugelot, Phys. Rev. C 20, 1085 (1979).
- <sup>29</sup>See AIP document No. PAPS PRVCA 23-2616-06 for 6 pages of center-of-mass cross section data. Order by PAPS number and journal reference from American Institute of Physics, Physics Auxiliary Publications Service, 335 East 45th Street, New York, New York 10017. The price is \$1.50 for microfiche or \$5 for photocopies. Airmail additional. Make checks payable to the American Institute of Physics.